Numerical Simulation of the Magnetic Bead Motion in a Micro Mixer for Cell Sorting

, , 7-3-1, E-mail: chainaro@thtlab.t.u-tokyo.ac.jp

, , 7-3-1, E-mail: fukagata@thtlab.t.u-tokyo.ac.jp

, , 7-3-1, E-mail: kasagi@thtlab.t.u-tokyo.ac.jp

Chainarong Chaktranond, Dept. of Mech. Eng., The Univ. of Tokyo, Hongo 7-3-1, Bunkyo-ku, Tokyo 113-8656, Japan

Koji Fukagata, Dept. of Mech. Eng., The Univ. of Tokyo, Hongo 7-3-1, Bunkyo-ku, Tokyo 113-8656, Japan

Nobuhide Kasagi, Dept. of Mech. Eng., The Univ. of Tokyo, Hongo 7-3-1, Bunkyo-ku, Tokyo 113-8656, Japan

Lagrangian particle tracking simulation is performed of the motion of magnetic beads in a micro serpentine mixer designed for cell sorting system. With time-dependent magnetic actuation, magnetic beads can be driven across the fluid streamlines and attach cells. Influence of magnetic forcing conditions (i.e., amplitude and frequency) on the mixer performance is examined.

1. Introduction

In regenerative medicine, efficient separation of specific cells from bio-fluid mixture, such as stem cells from blood/bone marrow, is of the greatest importance. One of the efficient separation techniques is called as the magnetic activated cell sorting (MACS). In MACS, the sample mixture and antibody-coated magnetic beads are mixed and the beads selectively attach the target cells by the antigen-antibody reaction, by which the target cells can be separated by using magnetic force. The major problems in the conventional MACS equipments are the long processing time and the high operation cost. Therefore, intensive research is being made for the development of micro-scale version of MACS, which may resolve the abovementioned problems.

One of the key issues for successful development of such a micro cell-sorting device is the mixing enhancement under low-Reynolds number environment. Therefore, a large number of micro mixers has been designed and developed. These can be classified into two groups: passive and active mixers. Active micro mixers use additional external forces for mixing. An advantage of active mixers is that the time and length of the mixer required for mixing are less than for passive mixer. In our group, Suzuki et al.[1] fabricated a micro serpentine mixer using time-dependent magnetic actuation. In this mixer, magnetic beads can move across streamlines of fluid and then attach to the cells by controlling magnetic actuation.

For the improvement of mixer performance, numerical simulation should be made in order to obtain detailed information, which cannot be accessed by experiment. Therefore, the objectives of the present study are to reveal the mechanism of mixing in the magnetic mixer of Suzuki et al.[1] with Lagrangian particle tracking simulations of the motion of magnetic beads and cells, and to find an optimal condition of magnetic actuation. The performance is evaluated by two mixing indices: the

largest Lyapunov exponents (λ) and the contact number (γ).

2. Computational model

2.1 Micro serpentine conduit

The dimension of mixer is shown in Fig. 1. One unit of the conduit is 160 μm long, 80 μm wide and 35 μm deep. In each mixer unit, four parallel magnetic conductors (labeled as 1 to 4) are embedded with equal spacing in the bottom wall. The conductors work to generate time-dependent magnetic force so that the immuno-magnetic beads move across the streamlines, as exemplified in Fig. 1b.

In the present simulations, we deal with a two-dimensional plane of that mixer, as shown in Fig. 2. We assume that the plane is located at 5 μm above the bottom wall, because Suzuki et al. observed in their experiment that the magnetic beads are accumulated on this plane. The mixer has a finite length and consists of nine units (denoted as Unit 1 to Unit 9). The flow direction is from left to right. The immuno-magnetic beads (displayed in blue) and the cells (red) are introduced, respectively, in the upper and lower halves of section A-A' in Unit 1. Initial positions of beads/cells within the section A-A' are given by uniform random numbers. The main body of the mixer, where the magnetic force is applied, extends from Unit 4 to Unit 8.

2.2 Lagrangian particle tracking

Trajectories of the beads and cells are computed by using one-way coupling Lagrangian particle tracking simulations in the above-mentioned two-dimensional plane. The fluid is assumed Newtonian and incompressible. The velocity field, which is stationary, is calculated by using the finite difference method on a regular grid system. The number of grids is 80 and 40 in the streamwise (x) and wall-normal (y) directions,

(a)
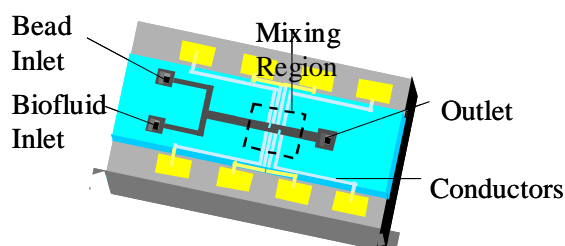
(b)
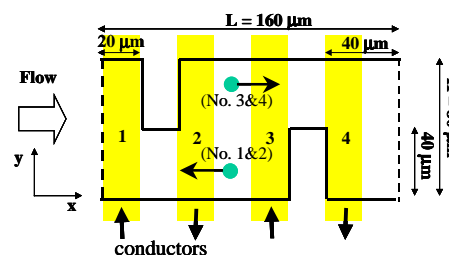
Fig. 1. Immuno-magnetic micro-mixer proposed by Suzuki et al. (2004).
(a) Overview of conduit; (b) Geometry and location of conductors in one unit.
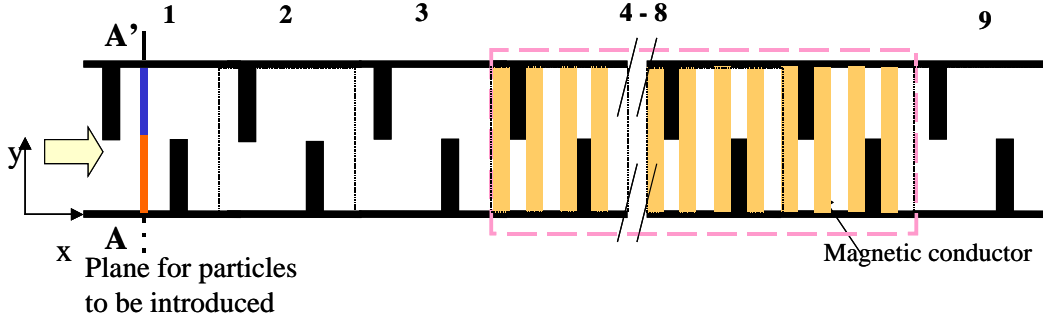
Fig. 2. Computational model.

respectively. The bulk Reynold is very low, i.e., $Re_b = U_b H/\nu = 0.0032$, where U_b is the bulk mean velocity, H is width of the mixer, and ν is the kinematic viscosity.

We assume for simplicity the beads and cells to be rigid spheres of 1 μm in diameter, although in reality cells are deformable and their typical diameter is on order of 10 μm. Brownian motion is neglected. Thus, the simplified particle equation of motion reads

$$\frac{d\vec{u}_p}{dt} = \frac{1}{\tau_p}\left(\vec{u}_f - \vec{u}_p\right) + \frac{\vec{F}_{mag}(\vec{x},t)}{m_p}, \qquad (1)$$

where $\vec{u}_p$ and $\vec{u}_f$ are, the velocity of particle and fluid, respectively, $\tau_p = \rho_p d_p^2/(18\mu_f)$ is the particle relaxation time, and $\vec{F}_{mag}(\vec{x},t)$ is the magnetic force. The quantities at the particle position, $\vec{u}_f$ and $\vec{F}_{mag}$, are interpolated from the grids by using the bilinear interpolation scheme. The time integration for the velocity and position of particles is done by using the Crank-Nicolson scheme.

Collisions among beads and among cells are neglected and only binary collisions between a bead and a cell are considered. When the distance between their center positions ($\vec{x_b}$ and $\vec{x_c}$, respectively) becomes less than the summation of their radii (r_b and r_c), i.e.,

$$\left|\vec{x_b} - \vec{x_c}\right| \le r_b + r_c, \qquad (2)$$

the bead is assumed to immediately attach the cell. Attachment of multiple beads to a single cell is allowed, similarly to actual situations. After a cell is attached by beads, the beads and the cell move together. To simplify the calculation of magnetic and drag forces, the cell combined with beads is treated as a single sphere with an equivalent diameter, mass and magnetic property.

2.3 Magnetic force

The magnetic forces are generated by the conductors embedded in the bottom wall of the mixer, as shown in Fig. 3. The conductors are assumed infinitely long and magnetic field, $\vec{H}$, is computed by the Biot-Savart law. The magnetic forces, $\vec{F}$, acting on a magnetic bead are

$$\vec{F} = \phi\mu_r\left(1 - N_d\right)V_m\left(\vec{H}\cdot\nabla\right)\vec{B}, \qquad (3)$$

where $\vec{B} = \mu_0\vec{H}$ is the magnetic flux density, μ_0 and μ_r are the permeability in vacuum ($\mu_0 = 4\pi\times10^{-7}$ H/m) and the relative permeability, respectively, V_m is the volume of magnetic bead, and N_d is the demagnetizing factor ($N_d = 0.333$ for a sphere). The relative permeability is a property of the magnetic bead. In this study, we assume

calboxyl-polystyrene ($\mu_r = 11.3$, $\rho_p = 1500$ kg/m^3), which is composed of percentage of iron oxide $\phi = 12$ %, as the material of magnetic beads, similarly to the experiment by Suzuki et al. [1]. This material is paramagnetic. Namely, the beads have no magnetic memory after removing the magnetic force.

The electric current is imposed on the conductors in the sequence of (4 & 1) → (1 & 2) → (2 & 3)→ (3 & 4), as shown in Fig. 3a, and these phases are referred to as Phase I to Phase IV. As an example, the distribution and directions of magnetic forces in Phase III are shown in Fig. 3b.
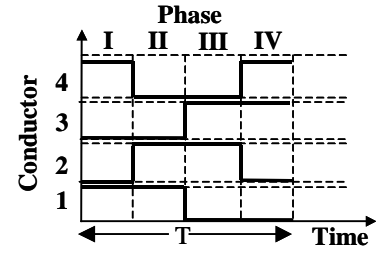
Fig 3a. Operation diagram of electric current.
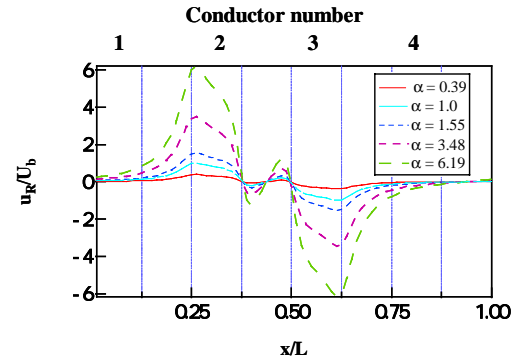
Fig. 3b Distribution of non-dimensionalized magnetic force in Phase III.

2.4 Actuation parameters

The actuation parameters in the present study are as the followings:

● **Strouhal number**

The Strouhal number, Str, is defined for the magnetic actuation. By using the frequency of the sequence of Phase I to Phase IV, f, and the distance between two conductors, $L/4$, the Strouhal number is defined as

$$Str = \frac{fL/4}{U_b} = \frac{L}{4U_bT}. \qquad (4)$$

- **Amplitude factor**

Because the particle relaxation time is extremely short, the magnetic force is nearly balanced by the drag force at any instants. Therefore, the maximum relative velocity between fluid and particle is $u_{R,\max} \simeq F_{\max}\tau_p / m_p$, where $F_{\max}$ is the maximum magnetic force. We define a non-dimensional amplitude of magnetic force, α, (hereafter referred to as the amplitude factor) as the ratio of $u_{R,\max}$ to U_b, i.e.,

$$\alpha = \frac{u_{R,\max}}{U_b} = \frac{F_{\max}\tau_p}{m_p U_b} . \qquad (5)$$

3. Results and Discussions

Efficiency of the mixer is evaluated under different conditions of magnetic force i.e., $\alpha = 0.39 - 6.19$ and $Str = 0.25 - 2$. The ratio of the number of beads to that of cells is unity. The area fraction of the particles (i.e., beads and cells) is about 3.2×10^{-3}.

As the measures for the mixer performance we computed the following quantities:

- **Lyapunov exponent**

The largest Lyapunov exponent, λ, is defined as

$$\lambda = \lim_{t \to \infty} \left[\frac{1}{t} \ln \frac{|d\boldsymbol{x}(t)|}{|d\boldsymbol{x}(0)|} \right], \qquad (6)$$

where t is time, and $|d\boldsymbol{x}(t)|$ and $|d\boldsymbol{x}(0)|$ represent the distance between two initially nearby points at initial time t and 0, respectively. This index indicates the average exponential rates of divergence (for positive λ) or convergence (for negative λ) of nearby points. In order to calculate this index, we use a method with reinitialization proposed by Sprott [2] and used by Suzuki et al. [1], Niu and Lee [3] and Deval et al. [4].

- **Contact number**

We define a contact number, n_c, as the number of cells attached by beads. By using this, we also define a contact ratio, γ, as the percentage ratio of the number of cells attached by beads to the total number of cells exiting from the outlet, N_c, i.e.,

$$\gamma = \left. \frac{n_c}{N_c} \right|_{outlet} \times 100 \ [\%] . \qquad (7)$$

Figure 4 shows typical effect of the magnetic actuation. Without magnetic actuation, the beads remain in the upper half even after long time. With the magnetic actuation, the beads move across the fluid streamlines and the mixing is enhanced. The global maximum of λ is found at $\alpha = 3.48$ and $Str = 1.4$, as shown in Fig. 5. Under some conditions, e.g., $\alpha = 0.39$, few beads can move into the lower half in spite of positive λ. In such cases, most of the beads are mixed only within the upper half, as shown in Fig. 6. This suggests that even if λ is positive, mixing between beads and cells is not necessarily good.

(a)

(b)
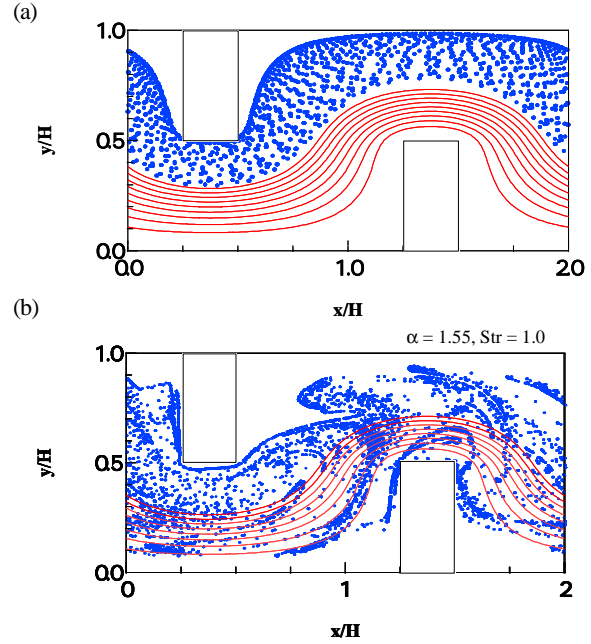
Fig. 4. Ensemble of bead positions in the region of magnetic conductors (unit $4-8$): (a) without magnetic; (b) with magnetic actuation at $\alpha = 1.55$, $Str = 1.0$.
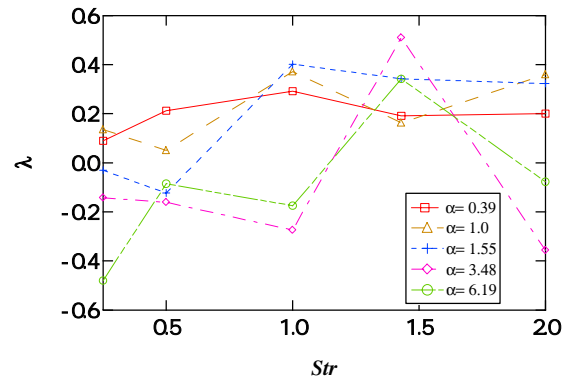
Fig. 5. Efficiency of mixing calculated by the largest Lyapunov exponent.
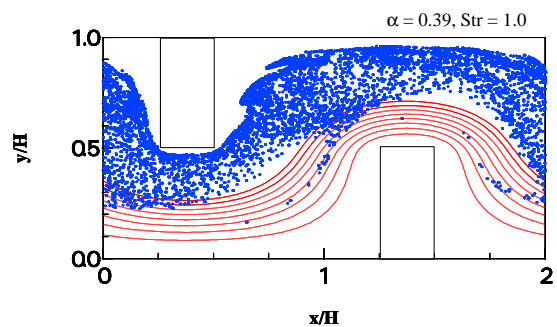
Fig. 6. Ensemble of bead positions in Phase I when $\alpha = 0.39$, $Str = 1.0$.
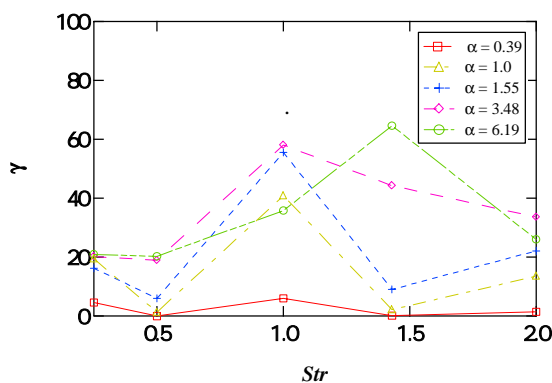
Fig 7. Efficiency of mixing measured by contact ratio

Figure 7 shows that when α is larger, γ is higher. The maximum values of γ are obtained at $Str = 1.0$, except for the case of α = 6.19 which gives the maximum value at $Str = 1.4$. With higher α, the beads should move further into the regions of cells but with the effect of inverse magnetic force around the inner edges of two conductors, as shown in Fig. 3b, the beads are trapped and accumulated around these regions.

In order to more explain the influence of magnitude and frequency of magnetic actuation on the motion of beads, we track the motion of 8 beads, which are evenly introduced in the upper half of the channel. Figure 8 shows that at α = 6.19 and $Str = 1.4$, motion of beads fluctuates into the lower half (solid line shows the interface line between bead and cell regions). This penetration results in the large value of γ.

At lower and higher Str ($Str = 1.0$ and 2), the trajectories of beads are close to each other. At $Str = 1.0$, long time of holding magnetic force ($T/4$) causes many beads to be trapped and accumulated near the conductors. At $Str = 2.0$, the short time causes beads to move forward and

backward into the positions which are near the previous time, i.e., a synchronization of the convection and the magnetic actuation. From Fig. 8c we can see that time for beads to be convected the half-length of one unit matches the holding time of two or more actuation phases. The beads are trapped around the conductors and released at the same timing. Therefore, their trajectories are similar. Under these conditions, when clustering beads attach to a cell, it results in low values of γ.

At α = 1.55 and $Str = 1$, beads gradually move across the interface line in downstream, as shown in Fig. 9. In the other word, the trajectories have mean drifts (or wave component much longer than the length of one unit), by which the beads deeply penetrate into the lower half. With this condition, beads can obtain a good dispersion, however, the length of mixer needs to be long enough.

Figure 10 shows the positions of beads first attaching to cells. At α = 1, the number of contacts gradually increases in the downstream units. Most of the contact positions are in the lower part of mixer (cell region). This is caused by the drifting, as mentioned above. For larger α, many of the contact positions are found in the upstream mixer units. The contact positions are mostly found in the bead-trapping regions. Few contact positions appear in the downstream because with the ratio number of beads to cell of unity, few free beads remain to attach to the cells.

4. Conclusions

We have numerically study the mechanism of mixing of beads and cells for cell sorting and the performance of a micro serpentine conduit using time-dependent magnetic actuation. The magnetic force conditions are in the range of $0.25 \leq Str \leq 2.0$ and $0.39 \leq \alpha \leq 6.19$.
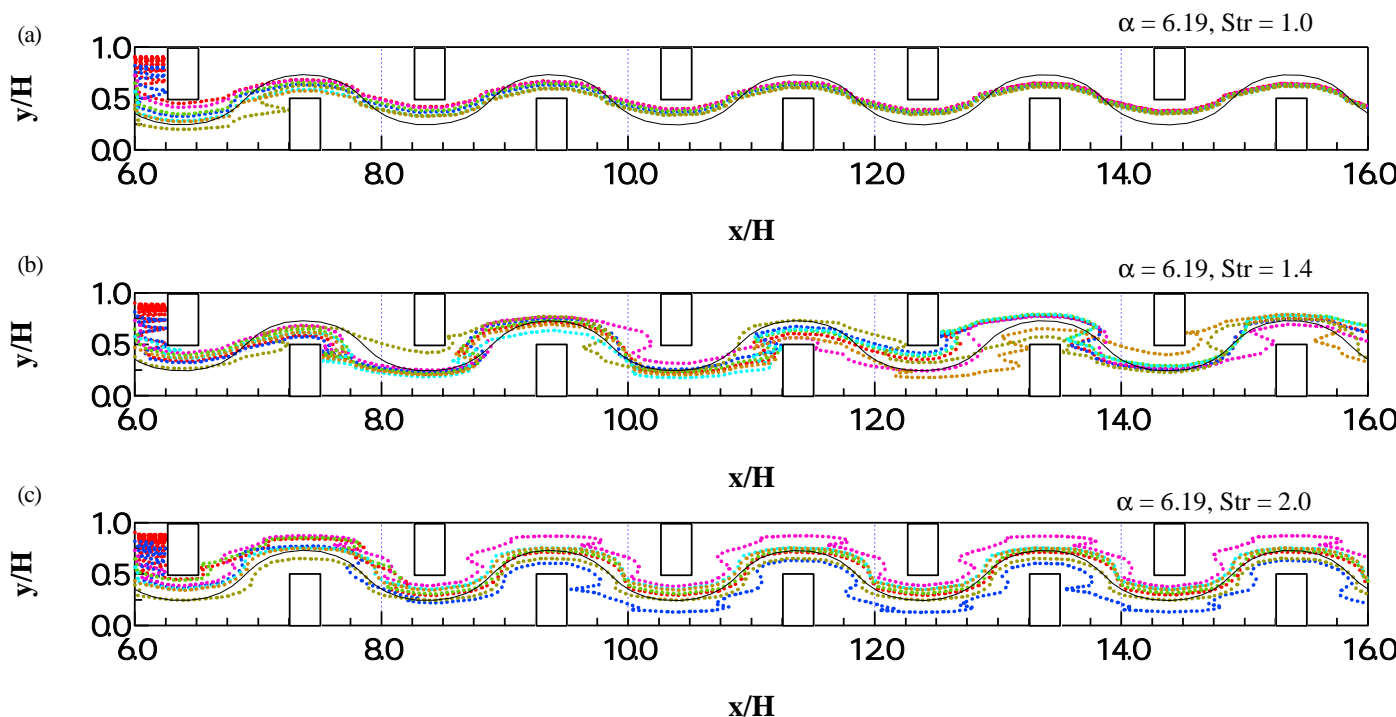
Fig. 8. Trajectories of beads at α = 6.19: (a) $Str = 1.0$; (b) $Str = 1.4$; (c) $Str = 2.0$.

$\alpha = 1.55, Str = 1.0$
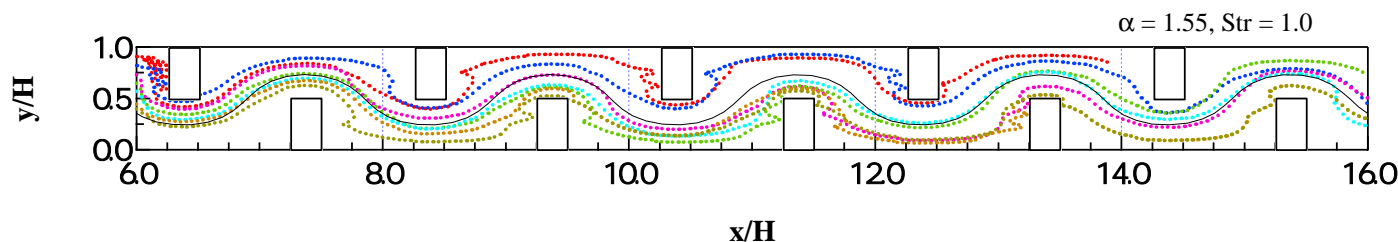
Fig. 9. Trajectories of beads at $\alpha = 1.0$ and $Str = 1.0$.

(a)

$\alpha = 1.0, Str = 1.0$

(b)

$\alpha = 6.19, Str = 1.0$
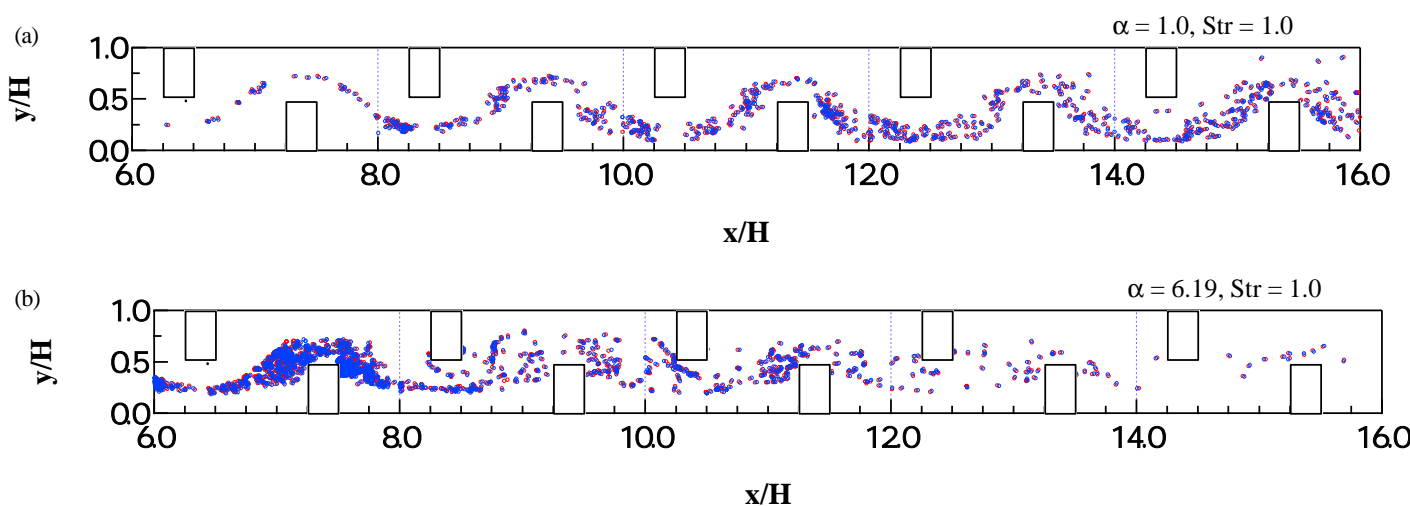
Fig. 10. Positions of first contact at $Str = 1$: (a) $\alpha = 1$; (b) $\alpha = 6.19$.

The simulation results reveal the mechanisms under various conditions of magnetic actuation. Assessment of the beads into the cell region depends on the relative velocity of beads increased by the magnetic force, i.e., $\alpha = u_R/U_b$. With $\alpha \sim 1$ and $Str = 1$, beads gradually access into the region of cells and a sufficient long length of mixer is required for deep access. The number of cells captured by beads increases as the increase of α. The Strouhal number of the magnetic actuation, Str, directly affects the dispersion of beads. A good dispersion is attained when $Str = 1.0$ except for the case with very large magnetic force, where the magnetic beads are trapped near the conductors.

Acknowledgments

References

(1) Suzuki, H., Ho, C.-M., and Kasagi, N., " A chaotic mixer for magnetic bead-based micro cell sorter," J. MEMS (2004), 779-790.

(2) Sprott, J. C., "Chaos and time-series analysis," Oxford University Press (2003), 116-117.

(3) Niu, X. and Lee, Y.K., "Efficient spatial-temporal chaotic mixing in microchannels," J. Micromech. Microeng. 13 (2003), 454-462.

(4) Deval, J., Tabeling, P., and Ho, C.H., "A dielectrophoretic chaotic mixer," In: Proc. IEEE Int. Conf. MEMS '02 (2002), 36-39.